A NUMERICAL STUDY OF JOULE HEATING EFFECT IN ELECTRODEPOSITION PROCESS-CASE OF COPPER ELECTRODEPOSITION

Watheq Naser Hussein[1a]*, Mohammed Ali Alshuraifi[2a], Bashar Abid Hamza[3a], and Raheem Aziz Hussein[4b]

Abstract: The electrochemical process in the presence of heat dissipation effect (Joule heating effect) is highly detected in practical electroplating solutions such as 0.6 M $CuSO_4$+0.5 M H_2SO_4 electrolyte, where currents passing through the cathode-anode-electrolyte increase temperature in the electrolyte and electrodes. Due to the complex nature of such systems and the diversity of physics describing it, a theoretical approach of appearance for natural convection on vertical and horizontal sides of a cathode in the presence and absence of Joule effect under unsteady state condition was observed using Comsol Multiphysics. It was found that the onset of natural convection on a vertical side depends on the Joule effect, and the time (t_n) for appearance is longer on the edges than in other areas. The horizontal side of a cathode assists the appearance of natural convection in the presence and absence of the Joule effect. The Rayleigh (Ra) number has larger values on the vertical side than the horizontal side due to the effect of surface concentration distribution C_s. A Sherwood, Sh-Ra mathematical relation such that $Sh=0.03Ra^{0.86}$ was proposed where natural convection had no pronounced effect on the deposition process. It was found that the Joule heating effect negatively affects the electrodeposition process by reducing the local current values.

Keywords: Natural convection, buoyancy, comsol, rayleigh

1. Introduction

Electrochemical deposition reduces metal ions of more than one metal (alloy) on a well-prepared conducting surface substrate to protect against corrosion or obtain some useful properties (Lowenheim, 1977). Accordingly, the electrodeposition process is a type of surface engineering activity.

Many factors affect the electrodeposition process, such as substrate morphology type, electrochemical properties, thermodynamic properties, and kinetic factors. Other factors affecting the solution-substrate interface include pH and temperature (Kanani, 2005; Lowenheim, 1977). In general, temperature can play several roles. The first is its effect on the solution through solubility, evaporation of the bath solution, stability of the solution constituents etc. The second effect is confined to the surface-solution interface, where increasing temperature increases the rate and efficiency of the electrodeposition process and reduces energy consumption (Gonçalves et al., 2021). The third relates to the electrodeposit properties, where previous studies suggest that increasing the temperature to 60^0C increases surface roughness or dendrite formation (Gonçalves et al., 2021; Jeon et al., 2022). Kwon et al. (2017) found that increasing temperature reduces the hardness of some deposits and increases the grain size.

It is known that an electrochemical process is a rate process, meaning that the oxidation or the anodic process and the reduction of ions are sensitive to the surface temperature and mass transfer effect (Al-Duaij et al., 2017; Paunovic, 2006). Many electrochemical depositions take place at approximately constant temperatures of about 30^oC. In electrodeposition, the works (pieces, load or cathode to be electrodeposited) is a batch process. As soon as a quantity of pieces is treated-electrodeposited, another quantity is served for the process in a sequence. Depending on the requirements, this could be done within a work shift or more. Large electrical current values are used depending on the work area (the current density is determined by dividing the total current by the total load area, which is commonly used in the electrodeposition field). Since the current path from the bus bar to the solution is variable, there will be a potential drop accompanied by a heating dissipating mechanism or Joule heating effect. Joule heating or Ohm's law (Diogo et al., 2013) is a phenomenon that accompanies the passing of a current in a conductor and is proportional to the conductor's resistance value.

Figure 1 shows the resistivity values for some electrodes used in electrochemistry (Diogo et al., 2013). Zinc, steel, and cadmium deposition with lower conductivity values than copper and aluminium are widely used in many electroplating systems. Therefore, Joule heating is expected to have more effect for the same current value, eventually increasing solution and deposit layer or surface temperature.

Authors information:

[a]Energy Engineering, Babylon University, Babylon, IRAQ. E-mail: met.watheq.naser@uobabylon.edu.iq[1]; met.bashir.abid@uobabylon.edu.iq[3]
[b]Chemistry, Wasit University, Alkut, IRAQ. E-mail: raheem_aziz2002@yahoo.com[4]
*Corresponding Author: met.watheq.naser@uobabylon.edu.iq
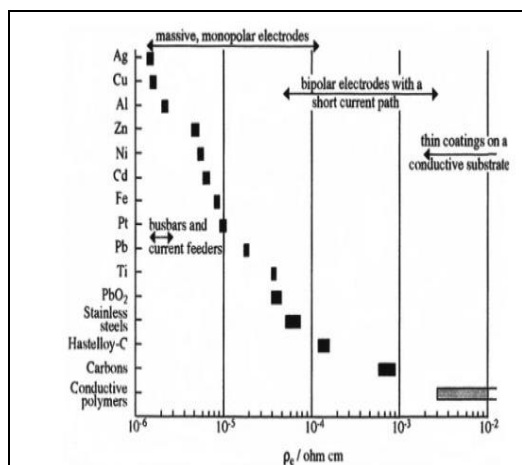
Figure 1. Resistivity of some electrodes (Diogo et al., 2013)

The process involves heat transfer between the electrodes or works and the solution, meaning the surface temperature is higher than the solution wherever the current is passing. Increasing the cathode surface's temperature in the presence of dissolved species affects concentration distribution. Due to the density effect, the ions are intensified near the bottom of the solution, imparting a poverty zone in the upper layers of the solution. Therefore, the current distribution is affected, especially when the kinetics are concentration-dependent. Density variation within the solution induces free convection. This variation is either due to localized heating or the distribution of dissolved species. Natural convection depends on the object geometry and temperature difference between the hot surface and the colder fluid (Selman et al., 1971; Amir et al., 2019).

Only a few studies consider the Joule heating effect on the electrodeposition process. Only the Laplace equation with heat transfer by conduction was solved without referring to the convection effect (Barvinschi, 2006). According to our knowledge, this is far from the industrial problem consideration regarding electrodeposition solutions. Schröter et al. (2002) showed that temperature gradient has a pronounced effect on convection near electrodes. Other concepts were used for other purposes (Hwang et al., 2019; Li et al., 2017). Other studies investigated conditions totally different from this study's focus and did not deal with complicated conditions (Selman et al., 1971; Amir et al., 2019; Kawai et al., 2009).

Natural convection appears due to the non-uniform density of the solution due to concentration or temperature differences. Therefore, in this study, a numerical approach was conducted to detect the Joule heating effect on the onset of natural convection via the concentration of the active species under an unsteady state process. The deposits' morphology, adherence, and porosity were not the subject of this study because these properties require experimental work and inspection. Unsteady state process best fits industrial applications, where the surface and solution temperature are variable as time proceeds, and

increasing solution temperature is accompanied by some risks. The cooling process to maintain the temperature within the desired range using a cooling coil or jacket adds complexities to the economic considerations.

This study assumed that: 1) the work received a constant value of current or current density (galvanostat); 2) the energy dissipation as heat (Joule effect) takes place only in the stagnant solution in absence of cooling process (i.e., insulated walls of the cell); 3) the evolution of deposit layer has no significant role in affecting the electrode's surface temperature (thin layer); 4) the anodes have a larger area than the cathode, therefore, their joule heat effects are negligible; 5) Cu^{+2} is electrodeposited on cathode as the main reduction reaction; 6) H^+ also is reduced on cathode; 7) the initial temperature of the solution is 303 K.

2. Numerical Simulation

The electrochemical system in this study is very complex. There are several ions with different diffusivities, concentrations and charge numbers. A system might not be adequately studied, and experimental work for obtaining the relevant variables is difficult due to interactions between diffusion and electro-migration flux, where both have the same direction. Moreover, there are more than two ions with different properties. This attribution conforms with (Volgin et al., 2009).

In this study, the Joule effect is used with applied current density on one side, and the other side is grounded. The general form handles and represents heat transfer (Holm and Jack, 2010).

$$\nabla(K\nabla T) + q = \rho c_p \frac{\partial T}{\partial t} \qquad (1)$$

For a constant thermal conductivity (within the range of temperatures estimated in this study and for ease of solution convergence), the following equation is used:

$$-\frac{q}{K} = -\frac{\rho c_p}{k}\frac{\partial T}{\partial t} + \nabla(\nabla T) \qquad (2)$$

We consider the copper plating process (composed mainly of 0.6 M CuSO4+0.5 M H2SO4) (Huang et al., 2019; Hussein, 2018) with an applied current density of 2 A/m^2 . The cathode dimension is 15x40 cm, as shown in Figure 2. Electrolyte conductivity was approximated to 55 S/m. Unsteady state, laminar, and weakly incompressible flow were considered. Hence, the following forms of the Navier–Stokes and continuity equations are applicable:

$$\rho\frac{\partial U}{\partial t} + \rho(U.\nabla)U = -\nabla P + \nabla.(\rho I + k) + F + \rho g \quad (3)$$

$$\rho\nabla.(U) = 0 \qquad (4)$$

$$k = \mu(\nabla U + (\nabla U^T)) \qquad (5)$$

The mass balance for the involved species can be represented by

$$\frac{\partial C_i}{\partial t} + \nabla J_i + U \nabla C_i = R_i \qquad (6)$$

$$J_i = -D \nabla C_i + Z_i \mu_{m,i} F C_i \nabla \theta_i \qquad (7)$$

Since the solution was composed of 0.6 M CuSO4+0.5 M H2SO4 with a dissociation degree of 0.31 for HSO4 (Sakr et al., 2013), the initial concentrations, c_{io}, for C^{+2}, H^+, SO_4^{-2}, and HSO_4 are 0.6, 0.65, 0.75 and 0.35, respectively. The flux at the electrode surface is (Kawai et al., 2009):

$$-D_1 \frac{\partial C_1}{\partial x} = \frac{j}{ZF}(1 - t_1 - t_2) \qquad (8)$$

The transference number is given by

$$t_i = \frac{C_{i0} Z_i \mu_i}{\sum_{i=1} C_{i0} Z_i \mu_i} \qquad (9)$$

Electroeutrality is also applicable inside the solution:

$$\sum C_i Z_i = 0 \qquad (10)$$

With zero velocity and no concentration effect, Equation 7 is reduced to

$$\nabla^2 \theta = 0 \qquad (11)$$

Equation 11 with appropriate boundary conditions can give the primary and secondary current distribution. The effect of mass transfer on current distribution is represented by tertiary current distribution:

$$j = j_0 C / C_b . \exp(-\eta / b_c) \qquad (12)$$

The flux of the deposition process for Cu^{+2} ion at the cathode is given by

$$D \frac{\partial C_{Cu+2}}{\partial \xi} = C_{Cu+2} / C_b . \exp(-\eta / b_c) / ZF \qquad (13)$$

where ξ is the normal direction to the surface.

Equation 12 is a modified Tafel equation used to estimate the mass transfer effect on current distribution. Using appropriate boundary conditions with the given values (Kawai et al., 2009), in addition to the Joule effect, Equations 3-12 also give velocity, temperature, and concentration distribution. It is assumed that the current value used in this study is less than the limiting current value.
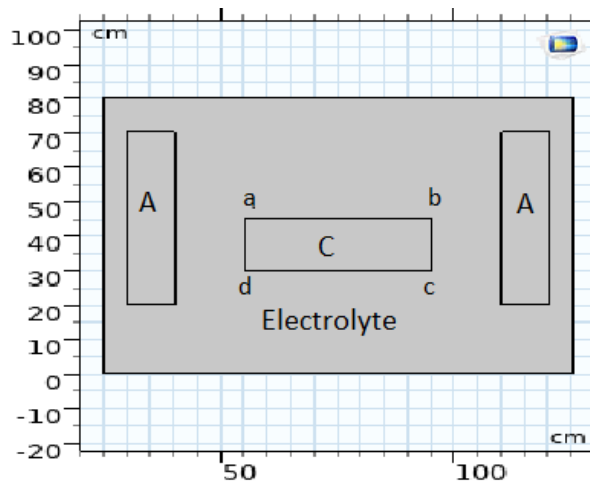
Figure 2. Configuration of the cell: A is the anode, and C is the cathode

Due to temperature variation within the solution, the relation of solution density to concentration can be represented by the linear expression in terms of solute concentration.

$$\frac{\rho_s - \rho_b}{\rho_b} = \sum_i^n \alpha_i (C_i - C_{ib}) \qquad (14)$$

where α_i is the densification coefficient (Kawai et al., 2009; Sakr et al., 2013) in m³/mol=0.14*10⁻³, 2.68*10⁻⁵,0 for Cu^{+2} and H^+, respectively and =0 for SO_4^{-2} and HSO_4.

The numerical simulation is approached using COMSOL 6 using time-dependent non-linear solver, element number of 9215. The parameters such as exchange current density and initial concentration can be found in (Hussein, 2018).

3. Results and Discussions

Many variables were used in this study, such as temperature distribution in the cell, solution velocity due to electrochemical process and temperature variation, concentration distribution for each active ion, diffusion layer, and temperature dependency. Considering all of them was tedious and needed much work that could be covered in more than one article. Therefore, a few limitations were introduced as necessary.

First, natural convection's appearance must be detected for both cases, with and without the Joule effect, as shown in Figure 3.
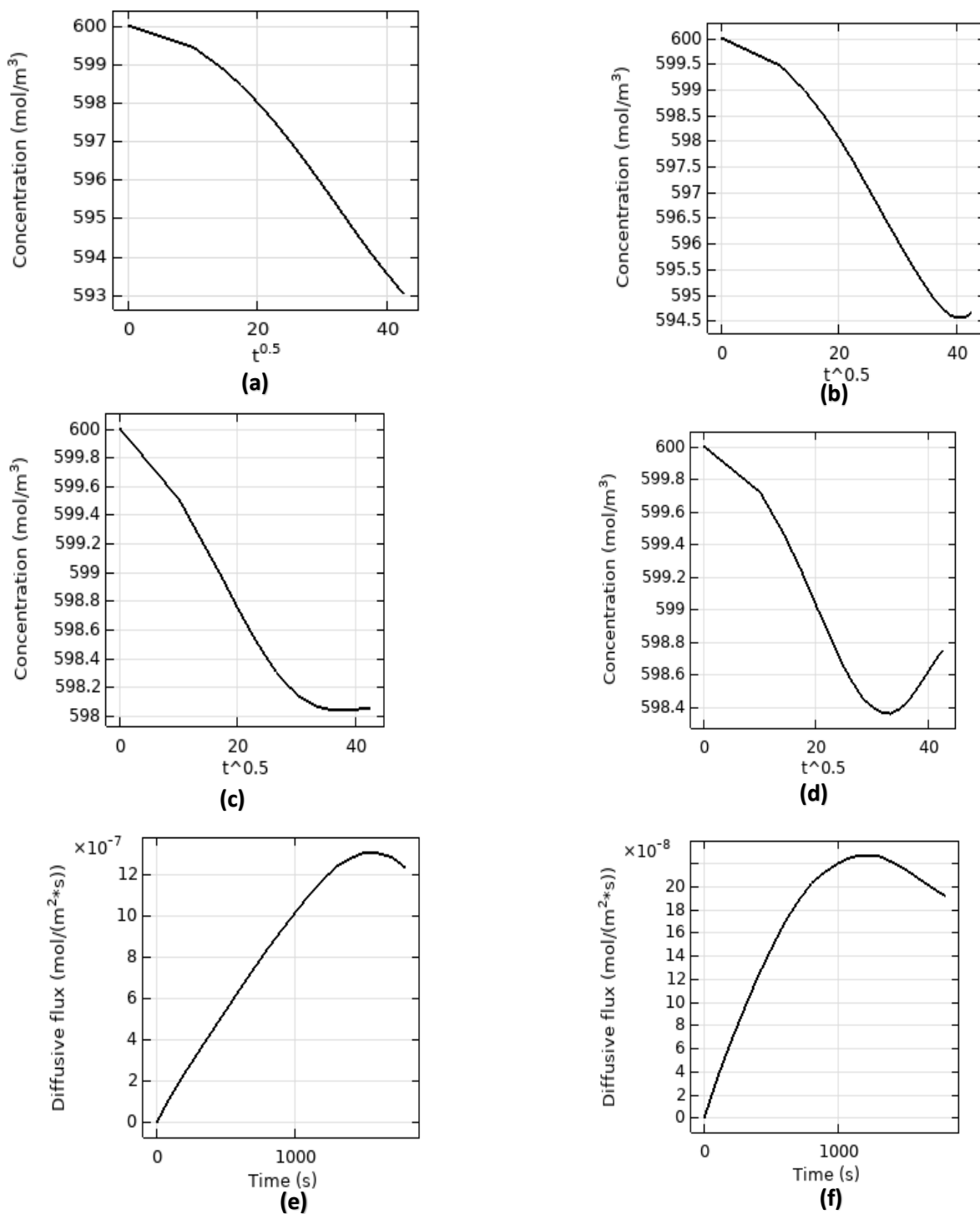
Figure 3. The onset of natural convection and diffusion flux: (a) without Joule effect at the midway of ad
(b) with Joule effect at the midway of ad (c) without Joule effect at the midway of cd (d). with Joule effect at the midway of cd (e)
diffusive flux at the midpoint of ad (f) diffusive flux at the midpoint of cd

Figure 3a and Table 1 show that natural convection is absent without Joule effect on the vertical surface along ad. The onset of natural convection on ad needs a longer time to appear near the edges of the electrode compared to Figure 3b and Table 1. In the early stages, the diffusion and migration mass transfer prevailed (Figures 3d-3e), and the Cu^{+2} ions reduction is proportional to $t^{0.5}$,

according to the Sand equation (Xuegeng et al., 2008). As time proceeds to a certain value, a deviation from linear to a quasi-steady state or equilibrium state of surface concentration is seen. At this stage, the buoyant force or natural convection becomes dominant. At the edges of the electrodes, the local current density intensified to a larger value than other points, and the

main component is the migration current. Accordingly, the edges needed a longer time for buoyancy to appear. In the case of the Joule effect, a higher temperature on the cathode surfaces created a graduated zone of temperature formation at the thermal boundary layer, assisting the appearance of buoyant forces, especially at the vertical electrode where the hot fluid motion was upwards against gravity. This behaviour coincided with the finding of (Xuegeng et al., 2008). The value differences are due to different cell configurations, process time, solution composition and temperature.

The onset of buoyant forces with and without the Joule effect on the horizontal cd surface was detected (Figures 3c and 3d) and could be attributed to increasing Archimedes force. The Archimedes force exceeded the viscous force at time t_n, leading to instability of the solution motion, where the force intensified in the vicinity of the surface ad. As the local current value increased, the time for the onset of buoyant force t_n also increased due to the reasons explained above. Table 1 gives the t_n values at a few positions of ad and cd.

Table 1. Time of natural convection onset at selected positions

Surface	Position on electrode (cm)	Value of t_n,(sec)$^{0.5}$ (δn, 10^{-5}m)	
		With Joule effect	without
ad	5	37 (22)	--------
	7.5	31.5 (19)	--------
	10	33 (16.5)	--------
cd	20	37 (13)	35 (12)
	10	36 (15)	34 (13)
	5	39 (21)	33 (19)

The critical Rayleigh number defined as the onset of natural convection, Ra_c is given by

$$Ra_c = g\delta_n(\rho_s - \rho_b)/\mu D \qquad (15)$$

Here, ρ_s and ρ_b are the density values on the cathode surface and at the bulk, respectively, δ_n is diffusion layer thickness at time t_n.
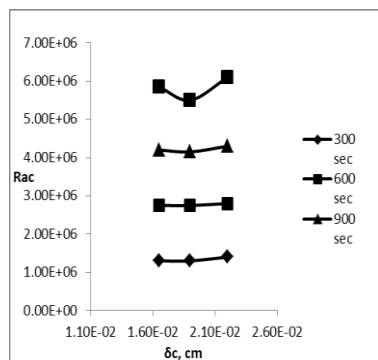
(a)
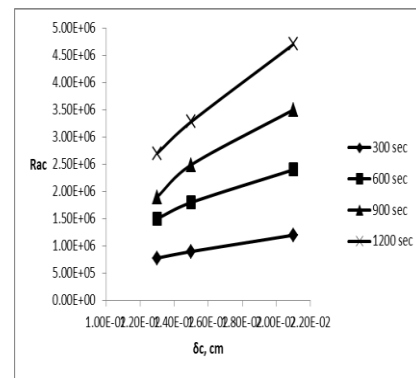
(b)
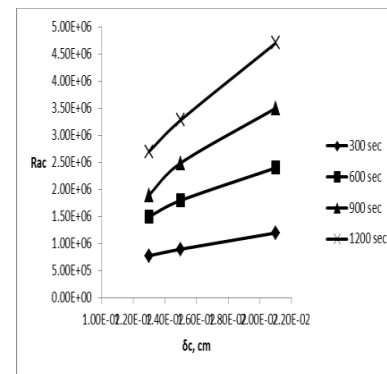
(c)

Figure 4. Relation of critical Rayleigh vs. critical diffusion layer at different time intervals:

(a) ad with Joule effect (b) cd with Joule effect (c) cd without Joule effect

Figure 4 shows that the Ra_c values are generally higher in the absence of the Joule effect on the horizontal surface cd (Figure 4 c), which can be attributed to the larger values of surface concentration. The Ra_c values are approximately stabilized along the diffusion layer on the ad surface (Figure 4a). At the same time, Rac increased with increasing diffusion layer and was proportional to increasing time on the cd surface. Ra_c enhancement is generally clearly pronounced in the absence of the Joule effect, attributed to the lower surface concentration (higher local current, Figure 5). According to Table 1, the diffusion layer formed adjacent to cd is lower in the absence of the Joule effect than in its presence (see also Figure 6). Figure 5 shows approximately the same shape as the results obtained by Kawai et al. (2009) and Xue Geng et al. (2008).
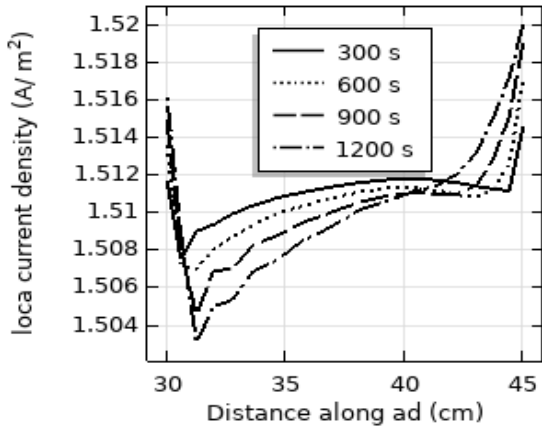
(a)
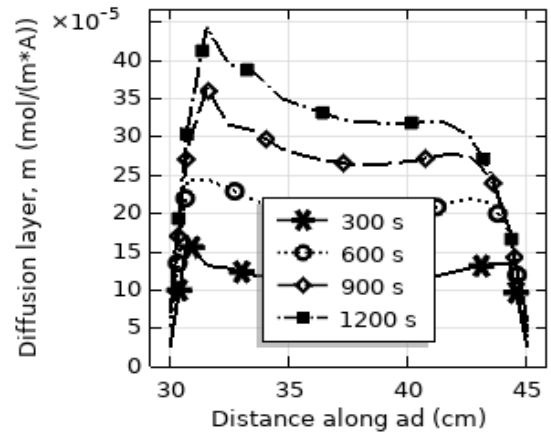
(b)
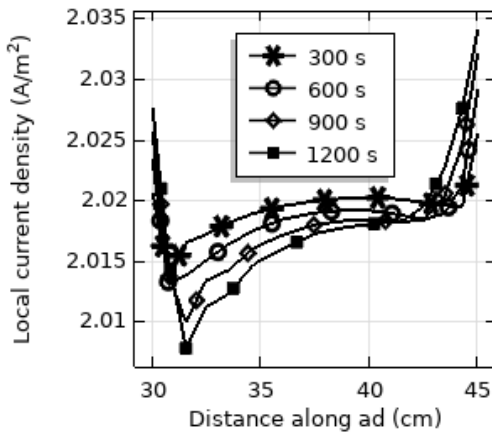
(b)
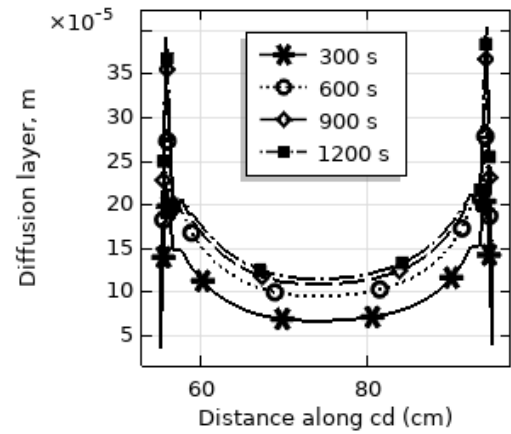
(c)

Figure 5. Distribution of local current on the ad:
(a) in the presence of the Joule effect (b) in the absence of the Joule effect

Figure 6 shows the boundary layer evolution on ad and cd in the presence and absence of the Joule effect.
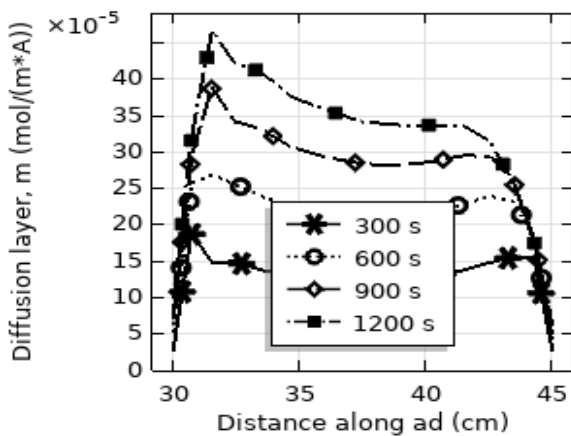
(a)
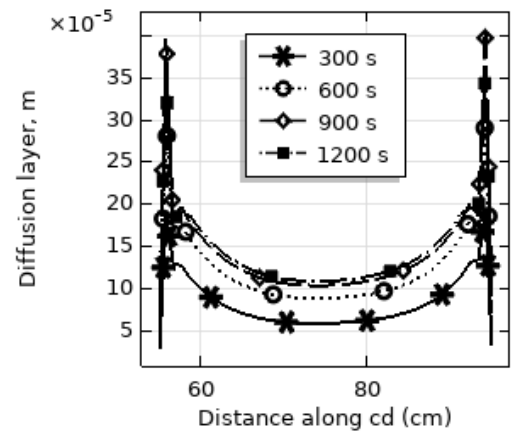
(d)

Figure 6. Evolution of diffusion layer δ: (a) with the Joule effect along ad starting from the bottom (b) without the Joule effect starting from the bottom along the same surface (c) with Joule effect along cd surface (d) without Joule effect along the same surface

Figure 6a shows that the diffusion layer values are uniformly distributed along the surface ad with increasing thickness as time proceeds due to the Cu^{+2} depletion. Figure 6b shows the same shape in the absence of the Joule effect, except that it is slightly lower than in Figure 6a. Figures 6c and 6d show the same trend for surface cd except for the thickness of the diffusion layer, where the Joule effect is slightly higher. This can be attributed to the larger amount of diffusive flux in the presence of the Joule effect or the temperature effect on the surface concentration distribution of Cu^{+2} ions and the resultant effect of viscous extension.

Rayleigh can be correlated to Sherwood number through analogy concepts (Sang-Hyuk and Deok-Woon, 2006), where the attained relation from Figure 7 is $Sh \approx 0.03 Ra^{0.86}$ for ad and cd, where

$$Sh = \frac{K.L}{D} \qquad (16)$$

$$K = \frac{(1-t)j}{nF(C_b - C_s)} \qquad (17)$$

Other relations can be found in (Duchanoy et al., 2000; Xue Geng et al., 2008).

Generally, Rayleigh has a higher value on the vertical side ad than cd with enhanced mass transfer value. This observation confirms the findings mentioned above.

The convective force increased along ad and cd surfaces as an exponential function while the diffusive flux decreased (Figures 3e-3f). Figure 8 shows the velocity field after 1000 sec, representing approximately the onset of buoyant forces (Table 1), where the vortices are gathered near the vertical surface from the bottom. The vortices increase as the time passes 1200 sec and so on.

Finally, Figure 9 shows the surface temperature plot, where the surface temperature facing the anode increases as time proceeds due to the Joule effect and has larger values than other areas.

(a)

(b)
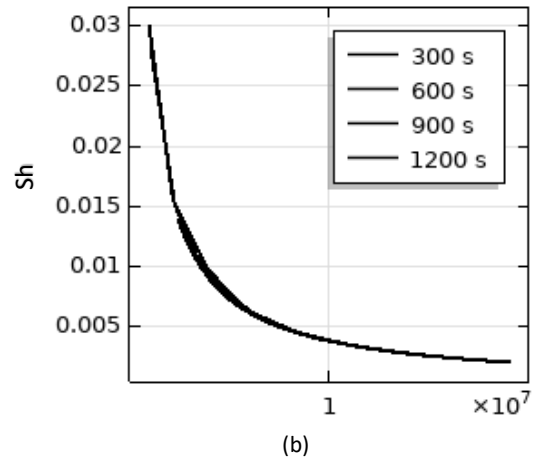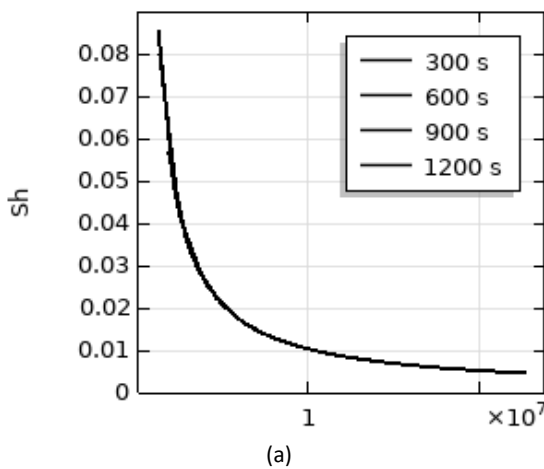
Figure 7. Sherwood-Rayleigh relationship: **(a)** ad surface **(b)** cd surface

(a)

(b)
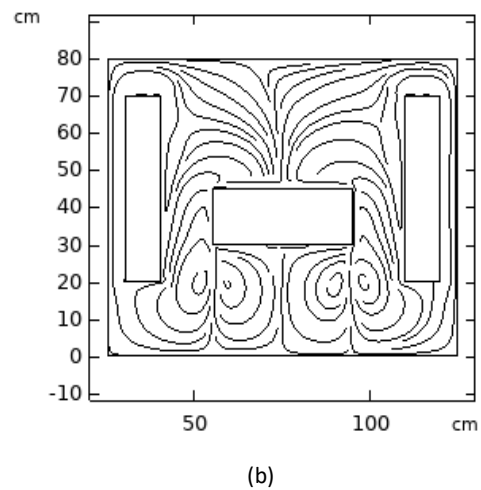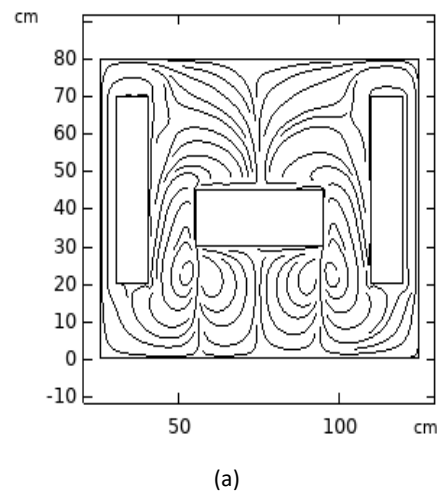
Figure 8. Velocity field after **(a)** 1000 sec **(b)** 1200 sec
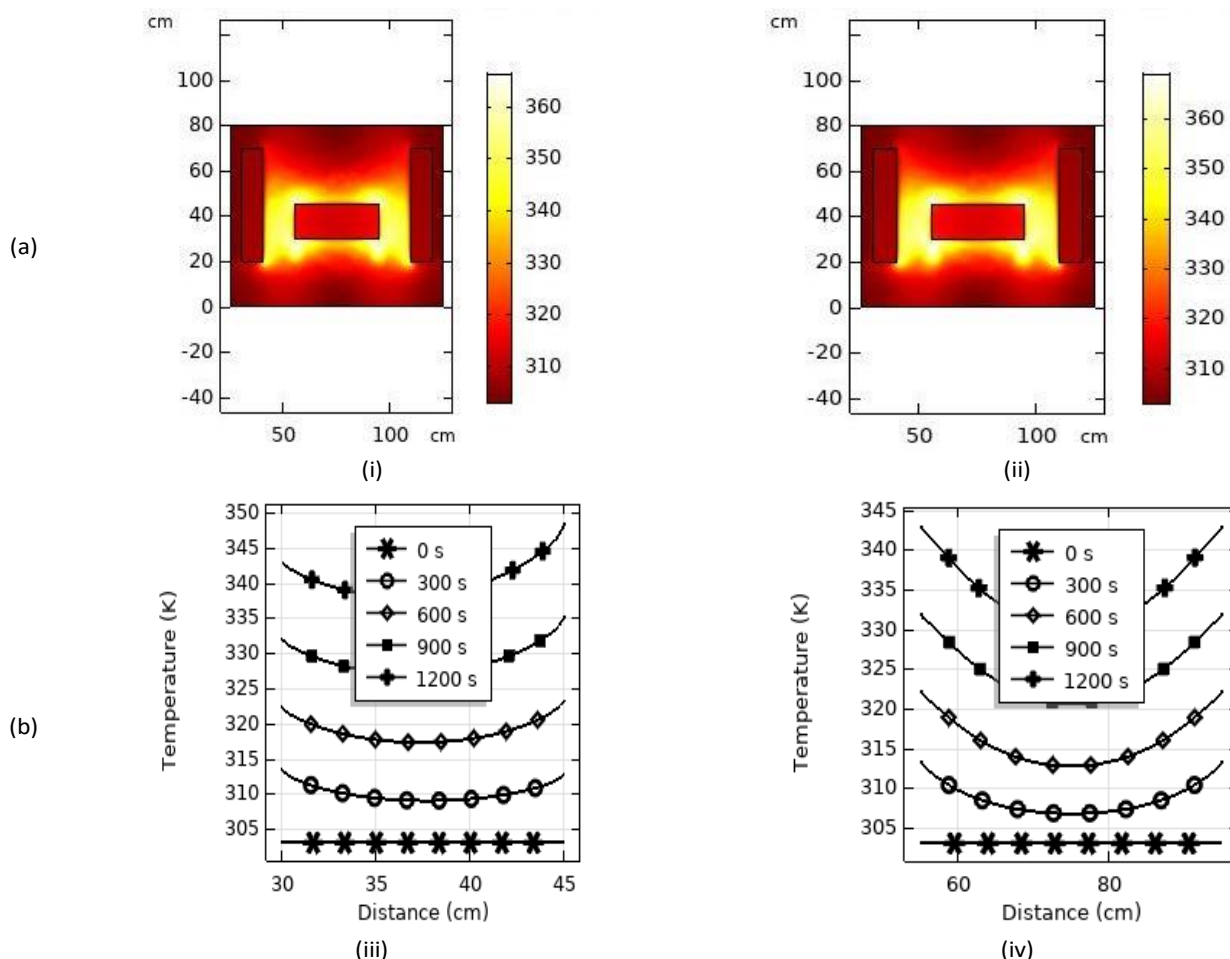
Figure 9. (a) Surface temperature plot: (i) after 1000 sec (ii) after 1200 sec
(b) Temperature plot: (iii) on ad (iv) on cd

5. Conclusion

In this study, based on the given working conditions:

1. The appearance of natural convection was detected on the vertical side in the presence of the Joule effect, while there is no such appearance in its absence.
2. On the lower side of the horizontal electrode, natural convection appeared both with and without the Joule effect.
3. Ra has larger values on the ad surface than horizontal cd.
4. The Sherwood relation with Ra is of an exponential form on both surfaces, ad and cd.
5. Natural convection took longer to appear on the parts receiving higher currents.
6. The solution temperature raised due to the Joule effect; it was smaller than on the cathode surface, in particular, the one facing the anode.
7. The onset of natural convection had a small effect on the electrodeposition process.
8. The Joule effect reduced the speed of the electrodeposition process due to lower current at the specified surface.

6. References

Ahmadkhaniha Donya, Ericso Fredrik, Zanella Caterina (2020) Optimizing Heat Treatment for Electroplated NiP and NiP/SiC, Coatings, 10: 1179.

Amir, Karimdoost Yasur, Mohsen, zadi, Hossein Hatemi (2019) Numerical Study of Natural Convection in a Square Enclosure Filled by Nanofluid with a Baffle in the Presence of Magnetic Field,, Iran. J. Chem. Chem. Eng 38: 209-220.

C. Duchanoy, F. Lapicque, C.F. Oduoza, A.A. Wragg(2000) Mass transfer and free convection associated with electrodeposition at long narrow upward facing tracks, Electrochimica Acta, 46: 433441.

Diogo M. F. Santos, César A. C.(2013) Hydrogen Production By alkaline water electrolysis, Sequeira Quim Nova. 36: 1176-1193.

F.A. Lowenheim (1977). Electroplating. McGraw-Hill, First Edition, 1977.

G. A. C. Gonçalves, P. M. S. Campos, T. C. Veloso, V. R. Capelossi (2021) Influence of current density and temperature in the zinc electroplating process at sulfate-based acid solution: study on process efficiency and coating morphology

Holman, P. Jack (2010) Heat Transfer. 9th ed. Published by McGraw-Hill Companies, Inc.

Hussein Watheq Naser (2018) A geometrical configuration and its effect on the performance of an electrochemical cell under free convection, Journal of Engineering Science and Technology, 13:3432-3444.

I.M. Sakr, W.A. El-Askary, A. Balabel,K. Ibrahim (2013) Numerical Study on natural and forced convection in Electrochemical Cells, CFD Letters, 5:120-131.

Jeon Joonyeob, Yoon Gil Ho, Vegge Tegs, Chang Jin Hyun (2022) Phase-Field Investigation of Lithium Electrodeposition at Different Applied Overpotentials and Operating Temperatures, Appl. Mater. Interfaces, 14: 15275–15286.

Jinjun Li, Xiaofei Lu, Feng Wu, Wei Cheng, Weidong Zhang, Shaoli Qin, Zhen Wang, Zhixiong You (2017) Electroplated Palladium Catalysts on FeCrAlloy for Joule-Heat-Ignited Catalytic Elimination of Ethylene in Air, Ind and Eng. Chem. Res, 56: 12520–12528.

 K. Sang-Hyuk, M. Deok-Woon, C. Bum-Jin (2006)Application of Electroplating Method For Heat Transfer Studies Using Anology Concept, Nuclear Engineering Technology,. 38: 251-258.

Kanani Nasser (2005). Electroplating: Basic Principles, Processes and Practice. Elsevier Science, 1st Edition.

Kwon, Hong-Beom, Kim, Kyong Tae, Ahn, Hye-Rin, Kim, Yong-Jun (2017) Electrodeposition and Characterization of Nanocrystalline Ni–B with Low Boron Content for MEMS Applications, Sensors and Materials, 29: 225-234.

M. Schröter, K. Kassner, I. Rehberg, J. Claret, F. Sagues (2002) Influence of ohmic heating on the flow field in thin-layer electrodeposition, Physical Review 66:1-6.

M. Huang, G. Marinaro, X.Yang, Fritzsche, B.Z. Lei, M. Uhlemann, K. Eckert, G. Mutschke (2019) Influence of ohmic heating on the flow field in thin-layer electrodeposition, Journal of Electroanalytical Chemistry 842: 203-217.

Milan Paunovic, Mordechay Schilesige (2006) Fundamentals of Electrochemical Deposition, 2nd edition, John Wiley & Sons, INC.

O.K. Al-Duaij, M.M. Abou-Krisha, M.I. Attia (2017) Influence of the Deposition Temperature on the Electrodeposition Mechanism of Zn-Co-Fe Alloy, Int. J. Electrochem. Sci. 12: 11972 – 11986

P. Barvinschi (2006) Numerical simulation of ohmic heating in idealized, Journal of Optoelectronics and Advanced Materials, 8:271-279.

S. Kawai, Y. Fukunaka, S. Kida (2009) Numerical Calculation of Transient Current Density Distribution along Vertical Plane Electrode in $CuSO_4 - H_2SO_4$ Electrolyte Solution, Journal of the Electrochemical Society, 157: F99.

Selman, Jan Robert, Newman, John (1971) Desalting by Means of Porous Carbon Electrodes, Journal of Electrochemical Society118: 510.

V.M. Volgin, A.V. Zhukov, G.N. Zhukova, A.D. Davydov (2009) Onset of natural convection in the electrochemical cell with horizontal electrodes under non-steady-state conditions: A numerical study, Russian Journal of Electrochemistry, 8: 1005.

Y. Xuegeng, E. Kerstin, H. Armin, U. Margitta (2008) The concentration field during transient natural convection between vertical electrodes in a small-aspect-ratio cell, Journal of Electronalytical Chemistry, 613: 97-107.